Microstructure evolution in base metal and welded joint of Grade 91 martensitic steels after creep at 500-600°C

F. Vivier[a], C. Panait[b], A.-F. Gourgues-Lorenzon[c], J. Besson[d]

Centre des Matériaux, Mines Paris, ParisTech, CNRS UMR 7633,
B.P. 87, 91003 Evry cedex, France

[a]florian.vivier@ensmp.fr, [b]clara.panait@ensmp.fr,
[c]anne-francoise.gourgues@ensmp.fr, [d]jacques.besson@ensmp.fr

Keywords : Grade 91, martensitic steels, microstructure, creep, welded joint, extractive replicas, microhardness, TEM, EDX analysis.

Abstract : The microstructure of Grade 91 base metal after long-term creep exposure at 600°C and after short-term creep exposure at 500°C was examined. Some cross-weld specimens extracted from a similar welded-joint were also tested at 500°C. After long term creep exposure (113431h) at 600°C, a decrease in microhardness was observed. TEM on carbon extractive replicas revealed chromium rich $M_{23}C_6$ carbides, MX-type precipitates, Laves phases and a small amount of modified Z phases. After short-term creep exposure (< 4317h) at 500°C, no evolution of microhardness or of precipitation was noted, compared to the as-received material. Fracture took place in the weld metal in all cross-weld specimens.

1. Introduction

The increase of steam temperature and pressure in fossil and nuclear power plants leads to the need of heat resistant steels with improved properties. ASME Grade 91 (modified 9Cr-1Mo) steel seems to be a good candidate for boilers and pressure vessel material for its high temperature strength and small thermal expansion coefficient. The further development of such steels needs a better understanding of their long-term microstructural evolution. There are rather few published data available on the microstructure of 9-12% Cr heat resistant steels for creep exposure times greater than 10^5h as well on the creep behaviour of the Grade 91 (base metal and welded joint) for temperatures lower than 600°C.

The purpose of this study is to bring more information on the microstructure of the Grade 91 after more than 10^5h of creep at 600°C, from 450h to 4317h at 500°C and on the creep behaviour of a Grade 91 welded joint at 500°C.

2. Experimental procedure

The testing parameters of creep specimens investigated in this study are given in table 1.

Creep-rupture tests on base metal were performed at 500°C in air on smooth cylindrical specimens with 81 mm length and 5 mm gauge diameter cut out from a large multipass welded plate of 70 mm in thickness. All specimens were subjected to a post weld heat treatment (around 750°C, 20h). Creep tests were also conducted at 500°C on cross-weld specimens.

A creep specimen with a rupture time of 113431h at 600°C was also studied to investigate long-time evolution of precipitation during creep. This creep specimen was cut out from a pipe, 121 mm in outside diameter and 20 mm in wall thickness.

The chemical composition and heat treatment of investigated steels are in good agreement with the ASTM specifications for Grade 91 steels [1].

	Temperature [°C]	Applied stress [MPa]	Time to rupture [h]	Elongation [%]	Area reduction [%]
1	500	310	450	22.1	83
2	500	300	511	17.2	84
3	500	290	1090	21.5	84
4	500	280	1546	14.3	85
5	500	270	4317	21.1	85
6	600	80	113431	7.3	37

Table 1: Investigated creep specimens

For the creep specimen tested for 113431h Field Emission Gun Scanning Electron Microscope (FEG-SEM) investigations were conducted on thin foils from the gauge part that were electropolished in an acid solution (45% acetic acid, 10% perchloric acid, 45% Butoxyethanol) at 40 V, -1°C. For the other specimens FEG-SEM investigations were carried out on bulk samples etched with Villela's reagent.

Creep damage was investigated by SEM on longitudinal cross sections of specimens. One broken part of the creep specimens were asymmetrically cut into two halves (i.e. quarters of "complete" specimens) by spark erosion. The half containing the specimen axis was used for metallographic examinations. A final mechanical-chemical polishing with colloidal silica was then carried out to reveal cavities without opening them, as chemical etching could have done. The size distribution of cavities was determined by image analysis of SEM images with a magnification of ×300 which was checked to reveal all cavities.

Transmission Electron Microscopy (TEM) investigations were carried out on carbon extractive replicas, prepared as follows. A carbon coating was evaporated on the polished and etched specimen and then the sample was immersed in a methanol solution with 1% HCl to detach the carbon layer from the specimen. Carbon replicas were recuperated on round copper grids.

For the creep specimen tested for 113431h several areas from 5 different extractive replicas were investigated and more than 400 precipitates were identified. The main purpose of TEM investigations on this creep specimen was to study the precipitation of modified Z phase. Literature reports an average diameter of MX precipitates of 20 to 40 nm [2]. MX precipitates of that size were identified in investigated extractive replicas, but extractive replicas are not adequate to study the density of these precipitates. Energy Dispersive X-Ray (EDX) analyses were conducted mainly on larger precipitates (average diameter higher than 90 nm).

For the other creep specimens TEM investigations were performed to give a complete characterization of the precipitation in the as received condition.

The chemical composition of precipitates was determined by EDX coupled with STEM observations and identified as follows: Cr–rich $M_{23}C_6$, Mo-rich Laves phase, modified Z phase (50 at.% (Cr + Fe) and 50 at.% (V+Nb)) and MX-type. Two kinds of MX precipitates were identified: V-rich VN and Nb-rich Nb(C, N).

3. Microstructure of as-received Grade 91 base metal

After the heat treatment (normalizing and tempering at around 1070°C and 760°C respectively), the microstructure exhibits prior austenitic grains filled with tempered martensite packets, blocks and laths.

Figure 1 shows the microstructure of Grade 91 base metal (a) and several types of precipitates that can be identified on carbon extractive replicas (b) : Cr-rich $M_{23}C_6$ carbides along prior grain and subgrain boundaries and fine MX carbonitrides within laths. EDX analyses of these fine precipitates reveal Nb-rich carbonitrides Nb(C,N) and V-rich nitrides VN (cf. **figure 2**).
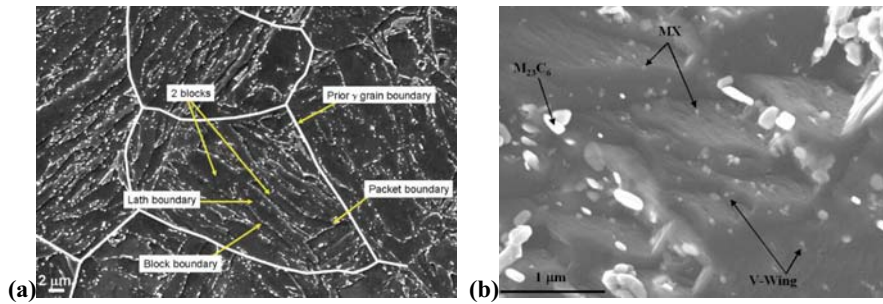
Figure 1: Typical microstructure and precipitates of as-received Grade 91 base metal (SEM)
(a) Villela etched bulk, some austenite grain boundaries are underlined in white
(b) Extractive carbon replica showing various kinds of precipitates

Nb(C,N), formed during solidification, is a preferential nucleation site for VN, appearing during tempering. Nb(C,N) inhibits grain growth and VN impedes dislocation motion, improving the creep strength. The mean sizes of $M_{23}C_6$ and MX precipitates are around 200 nm and 30 nm respectively. For this steel, the minimum size of identified MX particles seems to be about 20 nm.
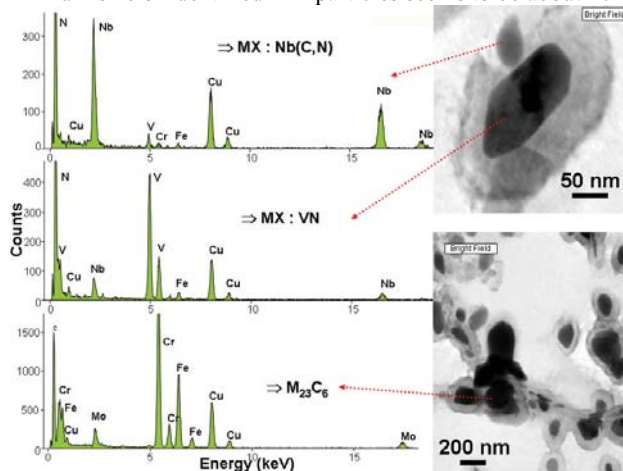
Figure 2: Identification of precipitates from replicas of Grade 91 base metal (EDX, STEM)

4. Mechanical properties of the creep specimens of base metal

4.1. Creep curves

Figure 3 shows the creep curves of the Grade 91 base metal at 500°C and 600°C. At lower applied stress, the secondary stage represents the majority of creep life. Modelling the creep behaviour of Grade 91 is still in progress. A Norton-type flow rule without damage law, but including internal stress and hardening, is able to modelling the first and second creep stages. The final stage, due to visco-plastic instability, leads to a predicted rupture time not very far from the experimental one.

(a)   **(b)**
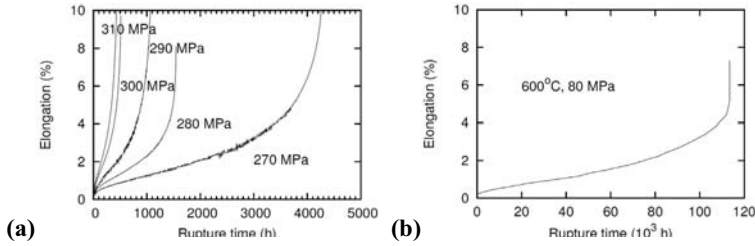
Figure 3: (a) Creep curves at 500°C, **(b)** Creep curve at 600°C

4.2. Fracture surfaces after creep at 500°C

Figure 4 shows fracture surfaces after creep tests, which revealed a transgranular ductile mode of fracture with dimples. Some Al_2O_3 inclusions (the biggest ones, up to 5 µm) and MnS (the smallest ones, up to 1 µm) were identified by EDX analysis in bigger dimples.
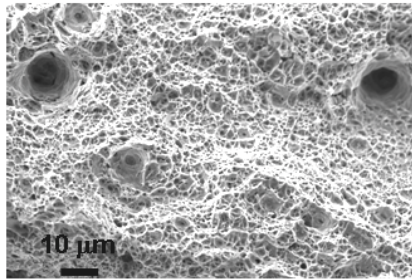
Figure 4: Fracture surfaces of crept base metal specimen after 4317h at 500°C (SEM)

4.3. Local microhardness after creep at 500°C and at 600°C

Figure 5 shows the evolution of microhardness along specimen axis from fracture surface to gauge length. The length has been normalized by the length of half-specimen ruptured after test. At 500°C, a slight decrease of hardness compared to that of as-received steel is measured away fracture surface. Close to the fracture surface, the hardness increases due to localised plastic deformation and hardening.

After long term creep exposure at 600°C, a significant decrease of hardness is observed along the gauge length of the specimen compared to the hardness of the as-received steel. Close to the fracture surface, hardness decreases strongly. This is to be related to creep damage development.
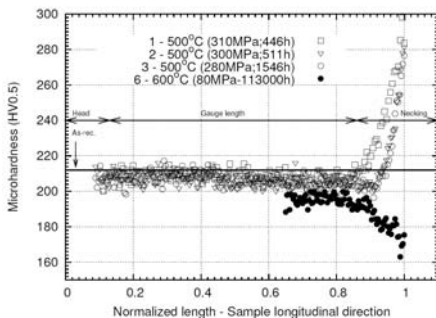
$$\text{Normalized length} = \frac{\text{Distance from fracture surface}}{\text{Length of specimen half}}$$

Figure 5: Evolution of hardness along the tensile direction in the investigated creep specimens

4.4. Damage development after creep at 500°C and at 600°C

For all specimens tested at 500°C, cavities were observed along specimen axis only in the necking area (cf. **figure 6a**), no cavity was observed away from the center of fracture surface, in contrary to crept sample at 600°C where cavities were observed throughout the gauge area (cf. **figure 7a**). **Figure 6b** presents the evolution of fraction of cavities along the specimen axis in two samples tested at 500°C. Some more seems to have developed after 1090h than 4317 h, nevertheless the fraction of cavities is lower than around 1%. So, damage is not very well developed after short time creep exposure at 500°C.

After long term creep exposure (113431h, 600°C), cavities were mainly located at boundaries and seemed to nucleate next to large precipitates such as Laves phases (cf. **figure 7b**). Because Laves phases are enriched in W, they can be easily observed using BSE images, which are sensitive to the mean atomic number of the precipitates.
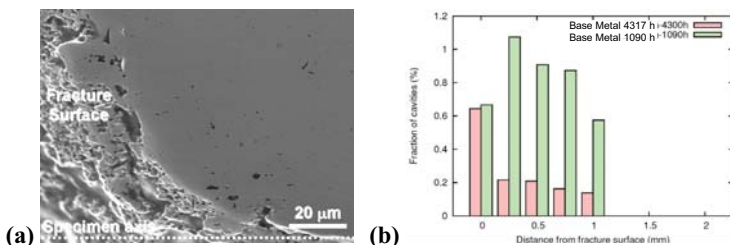
Figure 6: (a) Creep damage after short term creep exposure (4317h) at 500°C (SEM, SE);
(b) Evolution of the area fraction of cavities along the specimen axis at 500°C
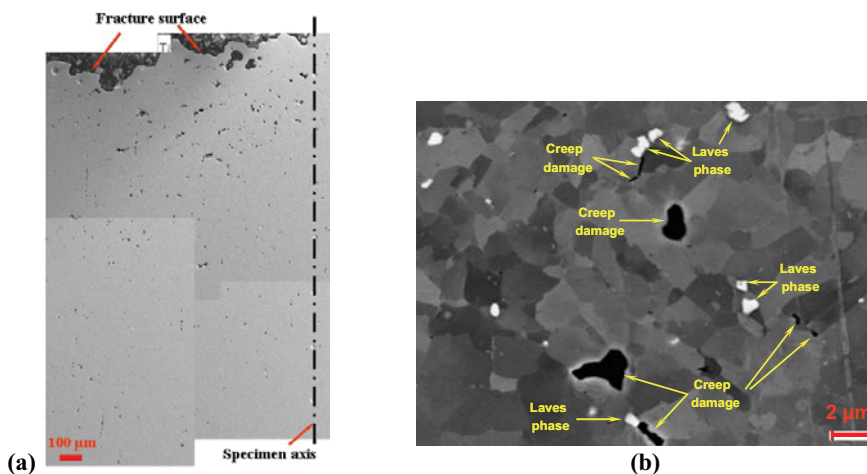
Figure 7: Creep damage and microstructure after long term creep (113431h) at 600°C
(a) Secondary electrons mode, SE; **(b)** Backscattered electrons mode, BSE

5. Microstructure of the base metal after creep

During creep exposure of the ASME Grade 91 steel there is a microstructural evolution of the steel: precipitation of new phases (Laves phases, modified Z-phases), coarsening of precipitates and recovery of dislocations in the matrix.

Laves phases are intermetallic phases, which precipitate during creep or aging. Their precipitation is observed after relatively short term (<4500h) creep exposure at 600°C [3], thus

decreasing the amount of Mo dissolved in the matrix, reducing solid solution strengthening. Laves phases have a significant growing rate during creep. Many aspects of characterisation of this phase have been studied in references [4, 5].

The modified Z phase is a complex (Cr,Fe)(Nb,V)N nitride. Its composition is 50 at.% (Cr + Fe) and 50 at.% (V+Nb) [6].

The precipitation of modified Z phases was also reported in the heat affected zone (HAZ) of welded joints after creep exposure at 600°C [7]. The modified Z phase precipitation occurs at the expense of MX precipitates, leading to their partial or complete disappearance and a decrease in MX-induced strengthening. For this reason, the modified Z phase precipitation can be dangerous for the service life of 9-12% Cr martensitic steels. The modified Z phase precipitation is much higher in the 11-12% Cr steels than in 9% Cr steels [6]. The Z phase precipitation is claimed to be the major cause of premature loss of creep strength of some 11-12% Cr heat resistant steels after relatively short term creep (<15 000h) [11]. For the ASME Grade 91 steel the effect of precipitation of modified Z phase on creep strength is not fully understood. To this aim, extractive replicas from specimen 6 were investigated with TEM.

The main purpose of TEM investigations was to determine the size and number density of modified Z phase particles in order to decide how to take into account the influence of this phase on the creep strength of the ASME Grade 91 steel. TEM investigations revealed a low number of modified Z phases compared to the size of the investigated area or the number of investigated precipitates. Only 13 precipitates out of 400 identified precipitates were found to be modified Z phases. The observed modified Z phases are large and widely spaced particles with a diameter of about 500 nm.
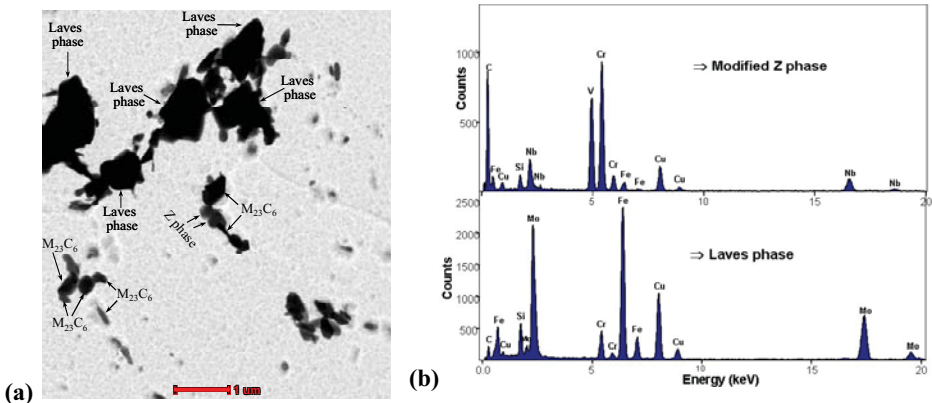
Figure 8 : **(a)** Precipitates in Grade 91 steel after creep at 600°C for 113431h
(TEM, bright field, extractive replica)
(b) EDX spectra for modified Z phases and Laves phase (TEM, extractive replicas)

Figures 9 (a) and **(b)** represent the microstructure of the ASME Grade 91 after 4317h of creep at 500°C and after 113431h of creep at 600°C, respectively. In **figure 9 (b)** the indicated precipitates could be identified by EDS in the FEG-SEM due to their large sizes. As it can be easily seen in **figures 8a** and **9b** the number and the size of Laves phases (almost micrometric size) are much higher than the number and size of modified Z phases. This suggests that Laves phase precipitation has a more significant influence on the creep strength loss of the steel than the modified Z phase precipitation.
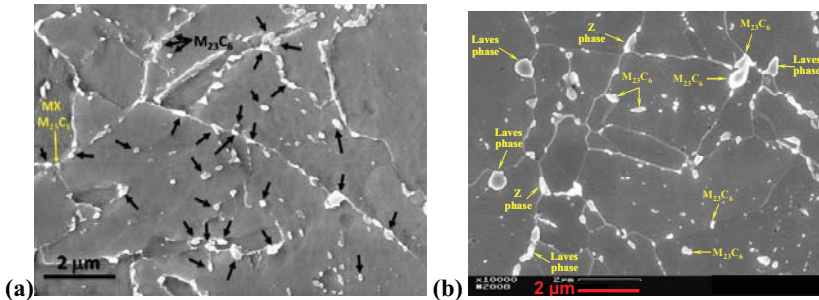
Figure 9 : Microstructure of ASME Grade 91 steel after creep (FEG-SEM, SE mode):
(a) at 500°C for 4317h (arrowed precipitates are all probably $M_{23}C_6$);
(b) at 600°C for 113431h

6. Microstructure of the welded joint after short-term creep at 500°C

Because of the welding heat cycles, various microstructures can be observed after a post weld heat treatment. Close to the fusion line, **figure 10** shows a heat affected zone (HAZ) composed by an area with coarse grains (CGHAZ) and an area with intercritical smaller grains (ICHAZ) close to the base metal. Between ICHAZ and CGHAZ a fine grain zone (FGHAZ) was denoted.
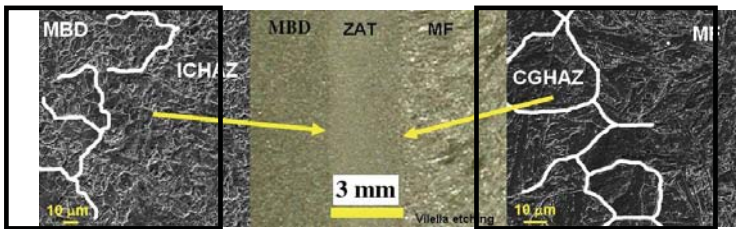
Figure 10 : Distribution of microstructure across the welded joint (Villela etching)

Some cross-weld creep specimens were extracted combining the two HAZ, the weld metal and a small part of base metal, perpendicularly to the weld axis. They were creep tested at 500°C for an applied stress from 210 MPa to 300 MPa. The main result of these creep tests is that fracture takes place in the weld metal, contrary to a reference creep test at 625°C where specimen classically fractured within ICHAZ [8,12]. **Figure 11** shows the evolution of fracture time for various levels of applied stress for specimens of base metal and welded joint.

The characterization of evolution of microstructure is in progress. Creep damage was localized close to the fracture surface, along the specimen axis. No cavity was detected next to the side surface.
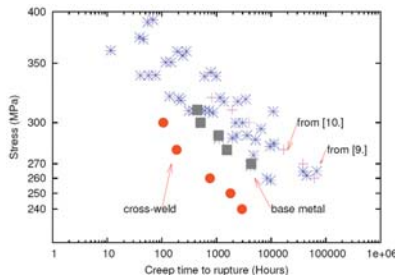
Figure 11 : Creep data at 500°C for base metal and welded joint [9, 10]
Solid symbols are for results of the present study

7. Conclusions and future work

New data have been brought about the creep behaviour of Grade 91 steel.

After creep for 113431h at 600°C, significant coarsening of existing precipitates, as well as intensive precipitation of coarse Laves phases and a low amount of modified Z phases were observed, together with damage cavities throughout the gage area and a significant decrease in hardness.

At 500°C, fracture takes place in the weld metal of cross-weld creep specimens. In base metal and in cross-weld specimens, fracture surfaces are ductile. Little creep damage was identified close to both the fracture surface and the specimen axis. Modelling of the creep curves is currently in progress. No significant precipitation of either Laves phase or modified Z phase was detected.

8. Acknowledgements

References

[1]   R. L. Klueh and D.R. Harries, *High-chromium ferritic and martensitic steels for nuclear applications*, July 2001, ASTM

[2]   P.J. Ennis, A.Czyrska-Filemonowicz, *Microstructural stability and creep rupture strength of the martensitic steel P92 for advanced power plant*, Acta Materialia, vol. 45, No.12, pp. 4901-4907, 1997

[3]   J. Hald, *Creep strength and ductility of 9 to 12% chromium steels*, Materials at high temperature 21 (1) 41-46

[4]   G. Dimmler et al., *Quantification of the Laves phase in advanced 9-12% Cr steels using standard SEM*, Materials Characterization 51 (2003) 341-352

[5]   Jae Seung Lee, et al., *Causes of breakdown of creep strength in 9Cr-1.8W -0.5Mo-VNb steel*, Materials Science and Engineering A 428 (2006) 270-275

[6]   H. Danielsen, J. Hald, *A thermodynamic model of the Z-phase Cr(V,Nb)N*, Computer coupling of phase diagrams and thermochemistry 31, 2007, 505-514

[7]   M.E. Abd El-Azim, A. M. Nasreldin, G. Zies, A. Klenk, *Microstructural instability of a weld joint in P91 steel during creep at 600°C,* Materials Science and Technology, 2005, vol. 21, no. 7, pp. 779-790

[8]   V. Gaffard, A.-F. Gourgues-Lorenzon, J. Besson, *High temperature creep flow and damage properties of 9Cr1MoNbV steels: base metal and weldment*, Nuclear Engineering and Design 235 (2005), pp. 2547-2562

[9]   K. Kimura, Proceedings of PVP2005, *Assessment of long-term creep strength and review of allowable stress of high Cr ferritic creep resistant steels*, July 17-21, 2005, Denver, Colorado USA

[10] NIMS, Creep Data Sheets No.53, June 2007

[11] T. Uehara, et al., Proceedings of the Conference on the "Materials for Advanced Power Engineering" (2002), pp. 1311-1320, Eds. J. Lecomte-Beckers et al., Forschungszentrum Jülich, Liège, ISBN 3-89336-312-2

[12] T. Watanabe**,** M. Tabuchi, M. Yamazaki, H. Hongo and T. Tanabe**,** *Creep damage evaluation of 9Cr–1Mo–V–Nb steel welded joints showing Type IV fracture*, International Journal of Pressure Vessels and Piping, Vol. 83, Issue 1, January 2006, pp 63-71